

Boundary effect and dressed states of a giant atom in a topological waveguide

Weijun Cheng,¹ Zhihai Wang,^{1,*} and Yu-xi Liu^{2,3}

¹Center for Quantum Sciences and School of Physics,
Northeast Normal University, Changchun 130024, China

²The Institute of Microelectronics, Tsinghua University, Beijing 100084, China

³Frontier Science Center for Quantum Information, Beijing, China

The interaction between the quantum emitter and topological photonic system makes the photon behave in exotic ways. We here study the properties of a giant atom coupled to two sites of a one-dimensional topological waveguide, which is described by the Su-Schrieffer-Heeger (SSH) chain. We find that the giant atom can act as an effective boundary and induce the chiral zero modes, which are similar to those in the SSH model with open boundary, for the waveguide under the periodical boundary. Except for the boundary effect, we also find that the giant atom can lift energy degeneracy inside the energy bands of the SSH chain and adjust spatial symmetry of the photon distributions for the states of the dressed giant atom and waveguide. That is, the giant atom can be used to change the properties of the topological environment. Our work may stimulate more studies on the interaction between matter and topological environment.

Introduction.—Topological physics, which was discovered in electronic systems [1, 2], has been widely promoted to photonic systems [3] for engineering and designing unconventional light behaviors. In the seminal work [4], the topological band structure was studied in photonic crystal with broken time-reversal symmetry. Afterward, various photonic systems were proposed to explore topological states of light, analog quantum Hall effects, synthetics of artificial gauge field, e.g., the two-dimensional photonic crystal structure in the microwave domain [5], coupled waveguides or resonators [6–9], exciton-polaritons [10], metamaterials [11]. Recently, the interaction between topological photonic system and quantum emitter attracts extensive attentions of the society [12–20].

The superconducting quantum circuits, which have high connectivity, flexible designability, easy controllability, and ability to reach strong light-matter coupling, provide a great platform to demonstrate topological physics [21–24] and realize topological photonic structure [25, 26], e.g., the Su-Schrieffer-Heeger (SSH) waveguide [27, 28]. The SSH waveguide is characterized by its non-zero winding number and zero-mode edge state(s) in the topological nontrivial phase with periodical and open boundary condition, respectively. By coupling to the quantum emitter, it furthermore emerges chirality [15]. In previous studies, the emitter was usually coupled to the waveguide via only one site. However, the transmon superconducting qubit, which serves as an artificial giant atom, can be engineered to couple with the waveguide via multiple sites. A key element in the giant atom scenario is that the photons in the waveguide travel back and forth between the coupling points, and the dynamics can be on demand adjust by tuning the size of the giant atom [29–41].

In this Letter, we study the interface between a giant atom and a one-dimension SSH waveguide. Here, the waveguide is considered under the periodical bound-

ary condition, but the giant atom induces an effective boundary. The boundary effect is manifested not only by the zero mode in the topological non-trivial phase of the waveguide, but also the bulk state inside the energy band. Moreover, our analytical results also demonstrate the chirality of the zero mode, the giant atom induced degeneracy lifted as well as the symmetry of the atom-waveguide dressed states. Moreover, in the topological trivial phase of the waveguide, we find a tunable dressed state which localizes in the energy gap when the giant atom is coupled to the waveguide within different sublattices. It implies that the giant atom will modify the topological nature of the waveguide.

Model and energy spectrum.—As schematically shown in Figs. 1 (a) and (b), we consider a two-level giant atom, with ground state $|g\rangle$ and excited state $|e\rangle$, which is coupled to a SSH chain waveguide via two sites. The interaction Hamiltonian of the SSH chain, formed by $2L$ resonators with the same frequency, is

$$H_{\text{SSH}} = \sum_{l=1}^L [t_1 \hat{C}_{A,l}^\dagger \hat{C}_{B,l} + t_2 \hat{C}_{A,l+1}^\dagger \hat{C}_{B,l}] + \text{H.c.}, \quad (1)$$

where $\hat{C}_{A(B),l}$ is the annihilation operator of the site A (B) in the l th unit cell. The coupling strengths are $t_1 = q(1 + \delta \cos \theta)$ and $t_2 = q(1 - \delta \cos \theta)$ with δ being the dimerization strength. The parameter θ can vary from 0 to 2π continuously. With the assistance of Fourier transformation $\hat{C}_{\alpha,l} = 1/\sqrt{L} \sum_k e^{ikl} \hat{C}_{\alpha,k}$, ($\alpha = A, B$) under the periodical boundary condition, the energy spectrum is obtained as $E_{k\pm} = \pm \omega_k$ with $\omega_k = \sqrt{t_1^2 + t_2^2 + 2t_1 t_2 \cos(k)}$. It should be noted that the spectrum is two-fold degenerate with $\omega_k = \omega_{-k}$. The topological property of the system is characterized by the winding number γ_{\pm} . As shown in the supplementary materials (SM) [42], $\gamma_{\pm} = 0$ for $t_1 > t_2$ ($0 \leq \theta < \pi/2$ and $3\pi/2 < \theta \leq 2\pi$) and $\gamma_{\pm} = 1$ for $t_1 < t_2$ ($\pi/2 < \theta < 3\pi/2$), corresponding to topologically trivial and topologically

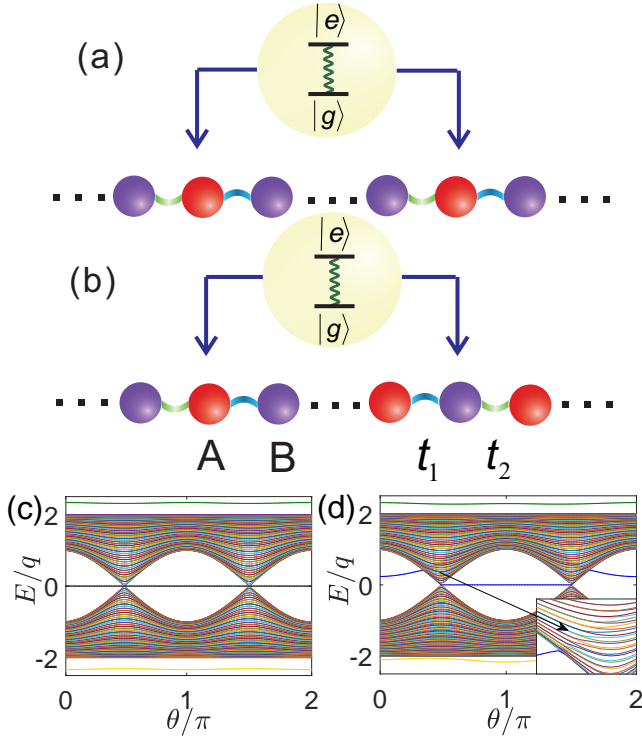


FIG. 1: Schematics of the SSH chain coupled to a giant atom via either A-A coupling in (a) or A-B coupling in (b). The energy spectrum versus θ in (c) for A-A and (d) for A-B coupling respectively under the periodical boundary condition. The parameters are set as: $L = 100$, $n = 50$, $m = 51$, $\delta = 0.5$ and $g = q$.

non-trivial phases, respectively. As for open boundary, the energy spectrum is numerically given in the SM [42] when there are odd and even sublattices respectively, where the zero-mode edge states are the signature of the topological nature of the system.

The interaction Hamiltonian between the giant atom and waveguide, in which the giant atom is coupled to the SSH chain via A-A (or A-B) coupling as shown in Fig. 1(a) (or Fig. 1(b)), is expressed as $H_{AA} = H_{\text{SSH}} + H_{I,AA}$ (or $H_{AB} = H_{\text{SSH}} + H_{I,AB}$) with

$$H_{I,AA} = g\sigma_+(C_{A,n} + C_{A,m}) + \text{H.c.}, \quad (2a)$$

$$H_{I,AB} = g\sigma_+(C_{A,n} + C_{B,m}) + \text{H.c.} \quad (2b)$$

Here, g is the atom-waveguide coupling strength, σ_+ is the raising operator of the giant atom, and n, m denote the number of the cells. Without loss of generality, we here set $n < m$. Moreover, we assume that the atom resonantly interacts with the bare resonator, and set their frequency to be zero as a reference.

In the single-excitation subspace, the energy spectra for H_{AA} and H_{AB} are numerically plotted as functions of θ under the periodical boundary condition in Figs. 1(c) and (d), respectively. For A-A coupling as shown in Fig. 1(c), the system is protected by the particle-hole

symmetry [43, 44] (if E is an eigenvalue of the Hamiltonian, then so is $-E$) and there is always a zero mode ($E = 0$) for arbitrary θ . Except for the zero mode and the bulk states inside the band, there are also two bound states, which locate outside the continual energy bands. Moreover, the giant atom lifts the two-fold degeneracy for all energy levels in upper and lower bands. For A-B coupling, the particle-hole symmetry is broken and the zero mode is absent in the topological trivial phase, but there is still an energy level in the gap. If the difference of $m - n$ is an odd (even) number, then as shown Fig. 1(d) and Fig. 2, with the variation of θ , this energy level connects to the upper (lower) energy band, where the two-fold degeneracy of the energy levels starts to be lifted (the detailed discussion is given in below). However, in contrast to the upper (lower) energy band, the two-fold degeneracy of the energy levels in the lower (upper) energy band is completely lifted for arbitrary θ . These numerical results can be verified analytically by the single excitation eigen-function

$$|\psi\rangle = U_e|e, G\rangle + \sum_k A_k \hat{C}_{A,k}^\dagger |g, G\rangle + \sum_k B_k \hat{C}_{B,k}^\dagger |g, G\rangle, \quad (3)$$

where $|G\rangle$ is the ground state of the SSH chain. Together with the Schrödinger equation $H|\psi\rangle = E|\psi\rangle$, we can obtain the eigen-energy E corresponding to $|\psi\rangle$. For A-A coupling, the eigen-energy E is given as

$$E = \frac{g^2}{\pi} \int dk \left[\frac{E(1 + \cos[k(m-n)])}{E^2 - \omega_k^2} \right], \quad (4)$$

which implies that $E = 0$ is always a solution. Moreover, if nonzero E is a solution, then so is $-E$, i.e., and the particle-hole symmetry is kept. For A-B coupling, it satisfies

$$E = \frac{g^2}{\pi} \int dk \left(\frac{E + Q}{E^2 - \omega_k^2} \right), \quad (5)$$

with $Q = t_1 \cos[k(m-n)] + t_2 \cos[k(n-m-1)]$. Equation (5) demonstrates that $E = 0$ is the solution only for $t_2 > t_1$, which is in the topological nontrivial phase ($\pi/2 < \theta < 3\pi/2$) [42]. Moreover, if a nonzero E is the solution, $-E$ is not. That is, the particle-hole symmetry is broken.

The nonzero energy level E^g in the gap (in topological trivial phase) for the A-B coupling can be tuned on demand by adjusting the size of the giant atom, that is, the value of n and m . In Fig. 2, we further show the energy spectrum for different $d = |m - n|$. As shown in Fig. 2(a)-(d), E^g is negative and positive for even and odd number d , respectively. Moreover, as the increase of d , the value of $|E^g|$ approaches to zero gradually. This can be understood from the expression of Q , which is an oscillation function of the wave vector k and d characterizes the oscillation frequency. Therefore, a large d

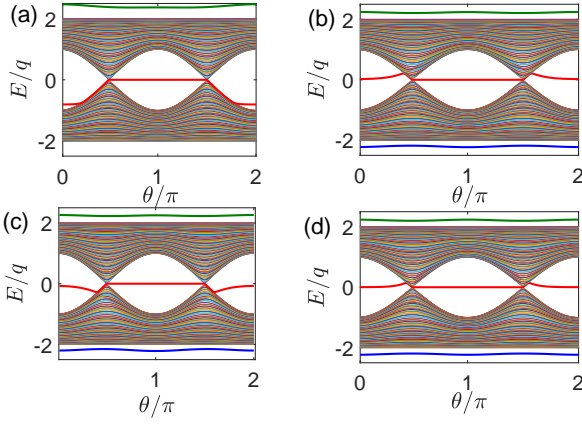


FIG. 2: The energy spectra for the A-B coupling. The parameters are set as: $L = 100$, $\delta = 0.5$ and $g = q$ and $d = |m - n| = 0, 3, 2, 5$ for (a), (b), (c), and (d), respectively.

naturally leads to a fast oscillation, and the contribution to the eigen energy can be neglected via integration. As a result, the eigen energy approaches to zero. More interestingly, for $d = 0$, that is, the giant atom couples to the waveguide via the same cell, the bound state which locates below the lower energy band disappears, as shown in Fig. 2(a). The numerical results show that the lowest energy is exactly the lower boundary of the energy band.

We have shown that the giant atom coupled to the SSH waveguide with periodical boundary condition will induce zero modes, which is similar to that of the SSH chain with open boundary. That is, the giant atom actually plays a role of the effective boundary. Such atom induced boundary effect also occurs when the waveguide is open, in which the zero mode localizes not only nearby the boundary of the waveguide, but also around the giant atom [42]. Recalling that the zero mode exists in the topological nontrivial phase in the SSH waveguide with the A-B open boundary condition (as shown in Fig. 1(d) in SM [42]) and comparing the above results with those of the SSH chain, we conclude that the topological nature of the SSH waveguide has been changed by the giant atom.

Zero mode and bound states.—In Fig. 3, we show the photonic spatial distributions for the zero mode and bound states, which are both the atom-waveguide dressed states, and bound states locate outside the upper and lower energy bands. Here, we focus on the topological nontrivial phase ($t_2 > t_1, \pi/2 < \theta < 3\pi/2$) and the physics for the topological trivial phase can be found in the SM [42]. In Fig. 3, the bars are the numerical results and the empty circles are the analytical results, which are obtains as follows.

The photonic distributions in the real space for the eigen state corresponding to the energy E can be given

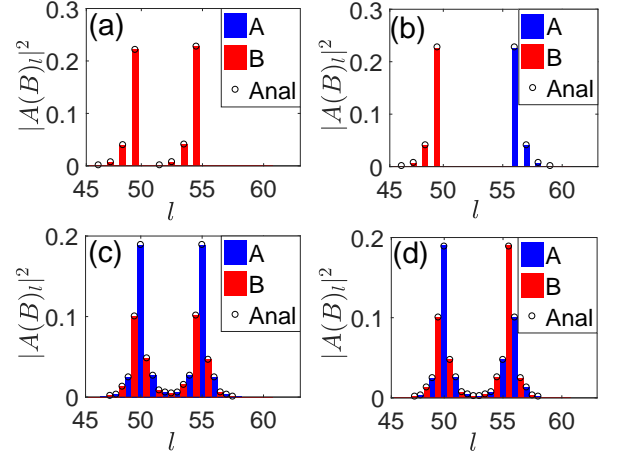


FIG. 3: The photon distribution of zero mode in (a) for A-A and (b) for A-B coupling. The photon distribution in the upper bound state in (c) for the A-A and (d) for the A-B coupling. The bars are numerical results and the empty circles are the analytical ones. The parameters are chosen as $L = 100$, $n = 50$, $m = 55$, $\theta = 0.8\pi$, $\delta = 0.5$ and $g = q$.

as (see SM [42] for details)

$$\frac{A_l}{U_e} = \frac{T}{\sqrt{x^2 - 4}} \left(a^{|l-n|} + a^{|l-m|} \right), \quad (6a)$$

$$\frac{B_l}{U_e} = \frac{A_l Y_1}{U_e T} + \frac{Y_2}{\sqrt{x^2 - 4}} \left(a^{|l-n+1|} + a^{|l-m+1|} \right), \quad (6b)$$

for the A-A coupling and

$$\frac{A_l}{U_e} = \frac{1}{\sqrt{x^2 - 4}} \left(T a^{|l-n|} + Y_1 a^{|l-m|} + Y_2 a^{|l-m-1|} \right), \quad (7a)$$

$$\frac{B_l}{U_e} = \frac{1}{\sqrt{x^2 - 4}} \left(T a^{|l-m|} + Y_1 a^{|l-n|} + Y_2 a^{|l-n+1|} \right), \quad (7b)$$

for the A-B coupling where $A_l(B_l)$ denotes the photonic amplitude in site $A(B)$ of the l th unit cell. We here define $T = gE/(Lt_1t_2)$, $Y_r = g/(Lt_{3-r})$ ($r = 1, 2$), $x = (E^2 - t_1^2 - t_2^2)/t_1t_2$, and $a = (x - \sqrt{x^2 - 4})/2$ for $x > 2$ or $a = (x + \sqrt{x^2 - 4})/2$ for $x < -2$.

For the zero mode corresponding to $E = 0$ in the topological non-trivial phase under the condition of the A-A coupling, Eqs. (6a) and (6b) are simplified to $A_l = 0$ and

$$\frac{B_l}{U_e} = Y_2 \times \begin{cases} (-\tau)^{-(l-n)} + (-\tau)^{-(l-m)} & (l < n) \\ (-\tau)^{-(l-m)} & (n \leq l < m) \\ 0 & (m \leq l) \end{cases}, \quad (8)$$

with $\tau = t_1/t_2$. Equation (8) shows that the photons only occupy sublattices B , whose label numbers for locating sites are smaller than m . That is, in the left side of the giant atom or between two coupling sites. However, for

A-B coupling, the eigen state of the zero mode can be derived from Eqs. (7a) and (7b) as

$$\begin{aligned} \frac{A_l}{U_e} &= Y_2 \times \begin{cases} (-\tau)^{(l-m)} & (l > m) \\ 0 & (l \leq m) \end{cases}, \\ \frac{B_l}{U_e} &= Y_2 \times \begin{cases} (-\tau)^{-(l-n)} & (l < n) \\ 0 & (l \geq n) \end{cases}, \end{aligned} \quad (9)$$

which shows that the photons occupy B(A) sublattices on the left (right) side of the giant atom and they satisfy the spatial symmetry $|A_r| = |B_{m+n-r}|$, but the sublattices between two coupling sites are not occupied. This has been clearly shown in Fig. 3(b). That is, the photon occupations for zero mode have chirality for both the A-A and A-B coupling.

For the two bound states, which locates outside the energy bands (except for the A-B coupling setup in the same cell, as discussed above), the photon distributions are lack of the chirality, as shown in Figs. 3(c) and (d), where the photonic distributions for the upper bound state are plotted for the A-A and A-B couplings, respectively. Figures 3(c) and (d) show that the photons occupy both of A and B sublattices in the chain, and occupation probabilities exponentially decay around the coupling sites between the giant atom and the waveguide. More interestingly, the bound states satisfy the spatial symmetry $|A(B)_r| = |A(B)_{m+n-r}|$ for the A-A coupling and $|A(B)_r| = |B(A)_{m+n-r}|$ for the A-B coupling, which can be observed from Figs. 3(c) and (d), also verified by analytical results in Eqs. (6a), (6b), (7a), and (7b).

States inside energy bands.—As shown in Figs. 1 and 2, the giant atom changes the energy-level structure of the SSH waveguide. Except for the emergency of zero modes and bound states, the bulk states inside two energy bands are also modified. When the giant atom is coupled, as shown in Fig. 4(a), the uniform distribution of photons in all sites of the SSH waveguide is changed to a sinusoidal way [42], which is similar to that in the SSH waveguide with open boundary. Moreover, as shown in Figs. 1 and 2, the giant atom with the A-A coupling lifts two-fold degeneracy of all bulk states for all parameters of the SSH waveguide, but the A-B coupling lifts degeneracy only in a certain parameter regime when the two coupling points are located in different sublattices.

To better understand the underlying physics behind the exotic degeneracy lifted in A-B coupling setup, we rewrite the Hamiltonian $H_{\text{SSH}} + H_{I,AB}$ as

$$\begin{aligned} H_{\text{SSH}} &= \sum_k [E_{k+}|E_{k+}\rangle\langle E_{k+}| + E_{k-}|E_{k-}\rangle\langle E_{k-}|] \quad (10) \\ H_{I,AB} &= \sum_{k,\sigma=\pm} [g_{k\sigma}|G\rangle\langle E_{k\sigma}|\sigma^+ + \text{H.c.}], \end{aligned} \quad (11)$$

in the momentum space, where

$$g_{k\pm} = \frac{g}{\sqrt{2L}} \left(\frac{\omega_k e^{ikn}}{t_1 + t_2 e^{ik}} \pm e^{ikm} \right). \quad (12)$$

It is clear $E_{k\pm} \gg |g_{k\pm}|$, thus the degree of freedom for the giant atom can be adiabatically eliminated [45–49]. Keeping up to the second order of the coupling strength $g_{k\pm}$, an effective Hamiltonian is derived as

$$\begin{aligned} H_{\text{eff}} &= \sum_{k,\sigma=\pm} E_{k\sigma} |E_{k\sigma}\rangle\langle E_{k\sigma}| \\ &+ \sum_{k,k',(\sigma,\sigma')=\pm} G_{k\sigma,k'\sigma'} |E_{k\sigma}\rangle\langle E_{k'\sigma'}|, \end{aligned} \quad (13)$$

with the coupling strength $G_{k\sigma,k'\sigma'}$, explicitly given in SM [42]. It shows that the giant atom will induce the virtual coupling between the bulk modes of the SSH waveguide with the same or different wave vector, inside the same or different bands.

For the parameters used in Fig. 1(d), a further numerical results show that $(|G_{k+,k'++}|, |G_{k-,k'-}|) \gg (|G_{k+,k'-}|, |G_{k-,k'++}|)$ and therefore the inter-band coupling can be neglected. Moreover, $|G_{k-,k'-}|$ is nearly flat except in the regime nearby $(k, k') = \pi$ as shown in Fig. 4(b). Therefore, for the lower band of the SSH waveguide, the giant atom only lifts the degeneracy [see Fig. 1(d)]. On the contrary, for $\theta = 0.4\pi$ around which the degeneracy starts to be lifted, we plot $|G_{k+,k'++}|$ in Fig. 4(c). It shows that the maximum value appears when $k + k' = 2\pi$. We note that, for the bare SSH waveguide, $E_{k+} = E_{(2\pi-k)+}$, therefore a strong effective coupling lifts the degeneracy. A further evidence can be found in Fig. 4(d), where the dependence of $|G_{k+, (2\pi-k)+}|$ on θ is plotted for different k . It shows that for $k = 1.1\pi$, the high peak of $|G_{k+, (2\pi-k)+}|$ appears at $\theta \approx 0.4\pi$ and $\theta \approx 1.6\pi$, where the degeneracy is lifted as shown in Fig. 1(d). For $k = 1.3\pi$ and $k = 1.5\pi$, the value of $|G_{k+, (2\pi-k)+}|$ is relatively small compared to the case for $k = 1.1\pi$, therefore the degeneracy is hardly lifted when the energy levels are far away from the lower boundary, which agrees with the energy spectrum in Fig. 1(d).

Discussion and conclusions.—In summary, we have studied the interaction between a giant atom and a topological waveguide, which is described by the SSH chain with periodical boundary condition. It can act as an effective boundary to induce a chiral zero mode when the giant atom is coupled to the waveguide via two sublattices of the same type and it lifts two-fold degeneracy of all bulk states for all parameters of the SSH waveguide. For the coupling to different types of the sublattices, we show that the zero mode appears in topologically non-trivial regime and there is a nonzero mode in the energy gap otherwise. Meanwhile, such coupling lifts two-fold degeneracy only in a certain parameter regime when the two coupling points are located in different sublattices.

In the microwave domain, the giant atom and the waveguide can be realized by the superconducting qubits (for example transmon) and the LC resonators. In such system, the coupling strength between resonators can achieve by 50 ~ 200 MHz for the existing technology [50–

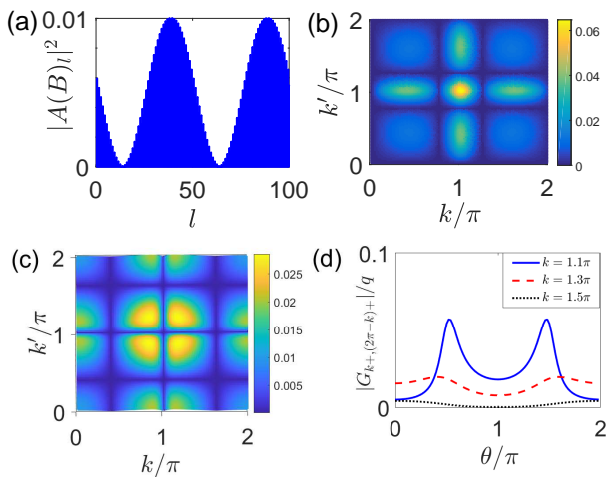


FIG. 4: (a) The photon distribution for the second top band energy level for $\theta = 0.8\pi$, $n = 50$, $m = 80$ in the case of A-A coupling. (b) and (c) are respectively $|G_{k-,k'-}|$ and $|G_{k+,k'+}|$ versus k and k' for $\theta = 0.4\pi$. (d) $|G_{k+,(2\pi-k)+}|$ versus θ for different k . The parameters for (b) (c) and (d) are $\theta = 0.4\pi$, $L = 100$, $n = 50$, $m = 51$ in the case of A-B coupling. The parameters shared by all of the figures are $\delta = 0.5$ and $g = q$.

[52]. Moreover, the periodical modulations of the nearest resonator coupling to obtain the SSH model has been already proposed using circuit superlattices [53]. The chiral and symmetry nature of the zero mode can be detected by introducing an auxiliary probing atom [42]. For the coupling strength 100 MHz between resonators and between the resonators and giant atom, the Rabi oscillation can still be observed [42] for the zero mode probing strength 10 MHz within the decay time $T_1 = 10 \mu\text{s}$ of the giant atom [54] for even larger decay rate of the probing atom.

In summary, we demonstrate the non-trivial light-matter interaction physics in the context of the topological waveguide QED. Our study is also possible to be experimentally realized in photonic and other solid state systems. The analytical treatment for 1D system lays a solid basis to understand the quantum effects in high-dimension topological waveguide systems and is helpful to further study the interaction between matter and topological environment.

Z. W. is supported by National Natural Science Foundation of China (Grant Nos. 11875011 and 12047566); Y. L. is supported by NSFC under Grant No. 11874037, and Key-Area R & D Program of Guangdong Province under Grant No. 2018B030326001.

* Electronic address: wangzh761@nenu.edu.cn

[1] M. Z. Hasan and C. L. Kane, Colloquium: Topological insulators, *Rev. Mod. Phys.* **82**, 3045 (2010).

- [2] X.-L. Qi and S.-C. Zhang, Topological insulators and superconductors, *Rev. Mod. Phys.* **83**, 1057 (2011).
- [3] T. Ozawa, H. M. Price, A. Amo, N. Goldman, M. Hafezi, L. Lu, M. C. Rechtsman, D. Schuster, J. Simon, O. Zeitlinger and I. Carusotto, Topological photonics, *Rev. Mod. Phys.* **91**, 015006 (2019).
- [4] F. D. M. Haldane and S. Raghu, Possible realization of directional optical waveguides in photonic crystals with broken time-reversal symmetry, *Phys. Rev. Lett.* **100**, 013904 (2008).
- [5] Z. Wang, Y. Chong, J. D. Joannopoulos and M. Soljačić, Observation of unidirectional backscattering-immune topological electromagnetic states, *Nature* **461**, 772 (2009).
- [6] M. C. Rechtsman, J. M. Zeuner, Y. Plotnik, Y. Lumer, D. Podolsky, F. Dreisow, S. Nolte, M. Segev and A. Szameit, Photonic Floquet topological insulators, *Nature* **496**, 196 (2013).
- [7] M. Hafezi, E. A. Demler, M. D. Lukin and J. M. Taylor, Robust optical delay lines with topological protection, *Nat. Phys.* **7**, 907 (2011).
- [8] H. Zhao, P. Miao, M. H. Teimourpour, S. Malzard, R. El-Ganainy, H. Schomerus and L. Feng, Topological hybrid silicon microlasers, *Nat. Commun.* **9**, 981 (2018).
- [9] M. Parto, S. Wittek, H. Hodaei, G. Harari, M. A. Bandres, J. Ren, M. C. Rechtsman, M. Segev, D. N. Christodoulides and M. Khajavikhan, Edge-mode lasing in 1D topological active arrays, *Phys. Rev. Lett.* **120**, 113901 (2018).
- [10] P. St-Jean, V. Goblot, E. Galopin, A. Lemaître, T. Ozawa, L. Le Gratiet, I. Sagnes, J. Bloch and A. Amo, Lasing in topological edge states of a one-dimensional lattice, *Nat. Photonics* **11**, 651 (2017).
- [11] W.-J. Chen, S.-J. Jiang, X.-D. Chen, B. Zhu, L. Zhou, J.-W. Dong and C. T. Chan, Experimental realization of photonic topological insulator in a uniaxial metacrystal waveguide, *Nat. Commun.* **5**, 5782 (2014).
- [12] J. Perczel, J. Borregaard, D. E. Chang, H. Pichler, S. F. Yelin, P. Zoller and M. D. Lukin, Topological quantum optics in two-dimensional atomic arrays, *Phys. Rev. Lett.* **119**, 023603 (2017).
- [13] R. J. Bettles, J. Minář, I. Lesanovsky, C. S. Adams and B. Olmos, Topological properties of a dense atomic lattice gas, *Phys. Rev. A* **96**, 041603 (2017).
- [14] S. Barik, A. Karasahin, C. Flower, T. Cai, H. Miyake, W. DeGottardi, M. Hafezi and E. Waks, A topological quantum optics interface, *Science* **359**, 666 (2018).
- [15] M. Bello, G. Platero, J. I. Cirac and A. Gonzalez-Tudela, Unconventional quantum optics in topological waveguide QED, *Science Adv.* **5**, eaaw0297 (2019).
- [16] C. A. Downing, T. J. Sturges, G. Weick, M. Stobińska and L. M.-Moreno, Topological phases of polaritons in a cavity waveguide, *Phys. Rev. Lett.* **123**, 217401 (2019).
- [17] L. Leonforte, A. Carollo and F. Ciccarello, Vacancy like dressed states in topological waveguide QED, *Phys. Rev. Lett.* **126**, 063601 (2021).
- [18] D. De Bernardis, Z.-P. Ciani, I. Carusotto, M. Hafezi and P. Rabl, Light-matter interactions in synthetic magnetic fields: Landau-photon polaritons, arXiv: 2009.05952 (2020).
- [19] M. Atala, M. Aidelsburger, J. T. Barreiro, D. Abanin, T. Kitagawa, E. Demler and I. Bloch, Direct measurement of the Zak phase in topological Bloch bands, *Nat. Phys.* **9**, 795 (2013).

- [20] S. de Léséleuc, V. Lienhard, P. Scholl, D. Barredo, S. Weber, N. Lang, H. P. Büchler, T. Lahaye and A. Browaeys, Observation of a symmetry-protected topological phase of interacting bosons with Rydberg atoms, *Science* **365**, 775 (2019).
- [21] X. S. Tan, D.-W. Zhang, Q. Liu, G. M. Xue, H.-F. Yu, Y.-Q. Zhu, H. Y., S.-L. Zhu, and Y. Yu, Topological Maxwell Metal Bands in a Superconducting Qutrit, *Phys. Rev. Lett.* **120**, 130503 (2018).
- [22] W. Cai, J. Han, F. Mei, Y. Xu, Y. Ma, X. Li, H. Wang, Y. P. Song, Z.-Y. Xue, Z.-Q. Yin, S. Jia and L. Sun, Observation of Topological Magnon Insulator States in a Superconducting Circuit, *Phys. Rev. Lett.* **123**, 080501 (2019).
- [23] W. Nie and Y. X. Liu, Bandgap-assisted quantum control of topological edge states in a cavity, *Phys. Rev. Research* **2**, 012076(R) (2020).
- [24] W. Nie, Z. H. Peng, F. Nori and Y. X. Liu, Topologically Protected Quantum Coherence in a Superatom, *Phys. Rev. Lett.* **124**, 023603 (2020).
- [25] P. Roushan, C. Neill, J. Tangpanitanon, V. M. Bastidas, A. Megrant, R. Barends, Y. Chen, Z. Chen, B. Chiaro, A. Dunsworth, A. Fowler, B. Foxen, M. Giustina, E. Jeffrey, J. Kelly, E. Lucero, J. Mutus, M. Neeley, C. Quintana, D. Sank, A. Vainsencher, J. Wenner, T. White, H. Neven, D. G. Angelakis, J. Martinis, Spectroscopic signatures of localization with interacting photons in superconducting qubits, *Science* **358**, 1175 (2017).
- [26] P. Roushan, C. Neill, A. Megrant, Y. Chen, R. Babush, R. Barends, B. Campbell, Z. Chen, B. Chiaro, A. Dunsworth, A. Fowler, E. Jeffrey, J. Kelly, E. Lucero, J. Mutus, P. J. J. O'Malley, M. Neeley, C. Quintana, D. Sank, A. Vainsencher, J. Wenner, T. White, E. Kapit, H. Neven, and J. Martinis, Chiral ground-state currents of interacting photons in a synthetic magnetic field, *Nat. Phys.* **13**, 146 (2017).
- [27] W. P. Su, J. R. Schrieffer and A. J. Heeger, Solitons in Polyacetylene, *Phys. Rev. Lett.* **42**, 1698 (1979).
- [28] X. Gu, S. Chen, Y. X. Liu, Topological edge states and pumping in a chain of coupled superconducting qubits, arXiv: 1711.06829 (2017).
- [29] A. F. Kockum, P. Delsing and G. Johansson, Designing frequency-dependent relaxation rates and Lamb shifts for a giant artificial atom, *Phys. Rev. A* **90**, 013837 (2014).
- [30] M. V. Gustafsson, T. Aref, A. F. Kockum, M. K. Ekström, G. Johansson and P. Delsing, Propagating phonons coupled with an artificial atom, *Science* **346**, 207(2014).
- [31] T. Aref, P. Delsing, M. K. Ekström, A. F. Kockum, M. V. Gustafsson, G. Johansson, P. J. Leek, E. Magnusson and R. Manenti, Quantum Acoustics with Surface Acoustic Waves, (Superconducting Devices in Quantum Optics, edited by R. H. Hadfield and G. Johansson, 2016).
- [32] R. Manenti, A. F. Kockum, A. Patterson, T. Behrle, J. Rahamim, G. Tancredi, F. Nori and P. J. Leek, Circuit quantum acoustodynamics with surface acoustic waves, *Nat. Commun.* **8**, 975 (2017).
- [33] A. Noguchi, R. Yamazaki, Y. Tabuchi and Y. Nakamura, Qubit-Assisted Transduction for a Detection of Surface Acoustic Waves near the Quantum Limit, *Phys. Rev. Lett.* **119**, 180505 (2017).
- [34] A. F. Kockum, G. Johansson and F. Nori, Decoherence-Free Interaction between Giant Atoms in Waveguide Quantum Electrodynamics, *Phys. Rev. Lett.* **120**, 140404 (2018).
- [35] G. Andersson, B. Suri, L. Guo, T. Aref and P. Delsing, Non-exponential decay of a giant artificial atom, *Nat. Phys.* **15**, 1123(2019).
- [36] A. Bienfait, K. J. Satzinger, Y. P. Zhong, H. S. Chang, M. H. Chou, R. G. Povey and A. N. Cleland, Phonon-mediated quantum state transfer and remote qubit entanglement, *Science* **364**, 368 (2019).
- [37] B. Kannan, M. Ruckriegel, D. Campbell, A. F. Kockum, J. Braumüller, D. Kim, M. Kjaergaard, P. Krantz, A. Melville, B. M. Niedzielski, A. Vepsäläinen, R. Winik, J. Yoder, F. Nori, T. P. Orlando, S. Gustavsson and W. D. Oliver, Waveguide quantum electrodynamics with superconducting artificial giant atoms, *Nature (London)* **583**, 775 (2020).
- [38] L. Guo, A. F. Kockum, F. Marquardt and G. Johansson, Oscillating bound states for a giant atom, *Phys. Rev. Research* **2**, 043014 (2020).
- [39] W. Zhao and Z. Wang, Single-photon scattering and bound states in an atom-waveguide system with two or multiple coupling points, *Phys. Rev. A* **101**, 053855 (2020).
- [40] X. Wang, T. Liu, A. F. Kockum, H.-R. Li and F. Nori, Tunable chiral bound states with giant atoms, arXiv: 2008.13560 (2020).
- [41] A. F. Kockum, Quantum optics with giant atoms—the first five years, arXiv:1912.13012 (2019).
- [42] See supplemental materials for the discussion of winding number of SSH model, the spectrum in the open boundary condition, the detailed calculation of the energy equation, the wave function and degeneracy lifted, the theoretically probed scheme for the chirality and symmetry of the zero mode and the energy spectrum for open SSH waveguide.
- [43] S. Ryu and Y. Hatsugai, Topological Origin of Zero-Energy Edge States in Particle-Hole Symmetric Systems, *Phys. Rev. Lett.* **89**, 077002 (2002).
- [44] L. Li, Z. Xu and S. Chen, Topological phases of generalized Su-Schrieffer-Heeger models, *Phys. Rev. B* **89**, 085111 (2014).
- [45] J. R. Schrieffer and P. A. Wolff, Relation between the Anderson and Kondo Hamiltonians, *Phys. Rev.* **149**, 491 (1966).
- [46] S. Bravyi, D. DiVincenzo and D. Loss, Schrieffer-Wolff transformation for quantum many-body systems, *Ann. Phys. (N.Y.)* **326**, 2793 (2011).
- [47] H. Fröhlich, Theory of the Superconducting State. I. The Ground State at the Absolute Zero of Temperature, *Phys. Rev.* **79**, 845 (1950).
- [48] S. Nakajima, Perturbation theory in statistical mechanics, *Adv. Phys.* **4**, 363 (1953).
- [49] Y. Li, C. Bruder and C. P. Sun, Time-dependent Fröhlich transformation approach for two-atom entanglement generated by successive passage through a cavity, *Phys. Rev. A* **75**, 032302 (2007).
- [50] S. Hacohe-Gourgy, V. V. Ramasesh, C. D. Grandi, I. Siddiqi and S. M. Girvin, Cooling and Autonomous Feedback in a Bose-Hubbard Chain with Attractive Interactions, *Phys. Rev. Lett.* **115**, 240501 (2015).
- [51] P. Roushan *et al.*, Spectroscopic signatures of localization with interacting photons in superconducting qubits, *Science* **358**, 1175 (2017).
- [52] R. Ma, B. Saxberg, C. Owens, N. Leung, Y. Lu, J. Simon and D. I. Schuster, A dissipatively stabilized Mott

- insulator of photons, *Nature (London)* **566**, 51 (2019).
- [53] T. Goren, K. Plekhanov, F. Appas and K. Le Hur, Topological Zak phase in strongly coupled LC circuits, *Phys. Rev. B* **97**, 041106 (2018).
- [54] M. Kjaergaard, M. E. Schwartz, J. Braumüller, P. Krantz, J. I.-J. Wang, S. Gustavsson and W. D. Oliver, Superconducting qubits: Current state of play, *Annu. Rev. Condens. Matter Phys.* **11**, 369 (2020).